

Density of states in multifragmentation obtained using the Laplace transform method

A. J. Cole

Laboratoire de Physique Subatomique et Cosmologie, Université Joseph Fourier CNRS-IN2P3, 53 Avenue des Martyrs, F-38026 Grenoble Cedex, France

(Received 8 February 2005; published 27 October 2005)

In equilibrium statistical mechanics, the density of microstates representing the statistical weight associated with a partition of an isolated system into subsystems (fragments) is the convolution of the state densities of the component subsystems. The Laplace transform approximation provides a simple representation of this density. Despite the fact that no external heat bath can be said to exist (the canonical ensemble is not appropriate) the approximation leads to partition probabilities that involve a product of factors (one for each fragment) expressed in terms of a characteristic inverse temperature. We apply the method to nuclear multifragmentation with particular emphasis on a transition that occurs when the major part of the available energy appears as kinetic (as opposed to internal excitation) energy of fragments. Finally, we discuss the shortcomings and advantages of expressing the weights of partitions with fixed total mass (charge) and multiplicity in a simple multinomial form.

DOI: 10.1103/PhysRevC.72.044605

PACS number(s): 25.70.Pq, 25.70.Mn, 24.60.Ky

I. INTRODUCTION

In the application of equilibrium statistical mechanics to isolated systems it is often useful to consider the density of microstates at energy, E , as a convolution of the densities corresponding to subsets of degrees of freedom. To this end we define the exact density,

$$\rho_{\text{ex}}(E) = \int_0^E \int_0^E \int_0^E \dots \delta\left(\sum_k E_k - E\right) \Pi_k[\rho_k(E_k) dE_k], \quad (1)$$

where the symbol Π_k denotes the product over subsets labeled by the subscript, k . Thus, for example, when a finite object breaks into fragments the microstate density is obtained as the convolution of fragment densities (possibly including motion of the centers of mass).

The numerical calculation of the convolution may be rather time consuming. In addition, the number of distinct sets of subsets may be rather large. For example, in the breakup of a parent system of mass, M , into fragments of mass $\leq M$, the number of distinct groups of subsets increases rapidly with increasing M (of order 2×10^8 for $M = 100$). It is therefore of interest to develop an approximation for the density $\rho_{\text{ex}}(E)$. The following section is devoted to this task and makes use of the Laplace transform [LT] approximation. In essence, the method involves making the Laplace transform of ρ_{ex} and then carrying out the inverse transform in an approximate manner, thus obtaining an approximation to ρ_{ex} (which we refer to as ρ_L). The technique is well known [1,2] and is included in Sec. II mainly to introduce appropriate notation.

We are especially interested in nuclear fragmentation [3–6]. In studies of this phenomenon use is often made of the hypothesis of independent emission [7]. Each fragment is emitted with a characteristic “one fragment” probability independently of all other emissions. This idea leads to a particularly simple product form for the probability [8] associated with any given fragmentation partition that is expressed as a product of Poisson distributions (the term *Poisson reducibility* has been

recently coined in works by Moretto and collaborators [9]). Thus, in terms of a set of parameters, $\{X_k\}$ each of which refers to a given fragment,

$$P(\mathbf{n}) = \text{const.} \Pi_k \frac{X_k^{n_k}}{n_k!}, \quad (2)$$

where n_k is the number of identical fragments associated with the label, k , and \mathbf{n} represents the partition vector $\mathbf{n} \equiv \{n_1, n_2 \dots n_k \dots\}$. A part of this work concerns an evaluation of the usefulness of Eq. (2) in the context of nuclear multifragmentation.

The expression that will be derived in Sec. II bears some resemblance to the density of states obtained using the canonical ensemble. This may well be misleading. The canonical result [10] is obtained by modifying the original system to include an additional set of degrees of freedom (representing the so-called heat reservoir). It is assumed that the reservoir is characterized by a microstate density, ρ_R , whose logarithm may be linearly expanded at energies close to the total energy of the combined system (E_R). Thus,

$$\ln[\rho_R(E_R - E)] = \ln[\rho_R(E_R)] - E/T_R \quad (3)$$

It is thus implicitly assumed that, for all configurations with nonnegligible probability, $E_R \gg E$, with the consequence that the limit of integration for E that should normally be E_R can be safely set to infinity. The convolution for the combined system now takes the form of the Laplace transform,

$$\begin{aligned} \rho_C(E_R) &= \rho_R(E_R) \int_0^\infty \left[\int_0^E \int_0^E \int_0^E \dots \right. \\ &\quad \left. \times \delta\left(\sum_k E_k - E\right) \Pi_k[\rho_k(E_k) dE_k] \right] e^{-E/T_R} dE \\ &= \rho_R(E_R) \Pi_k \left[\int_0^\infty \rho_k(E_k) e^{-E_k/T_R} dE_k \right] \\ &= \rho_R(E_R) \Pi_k [Z_k(T_R)]. \end{aligned} \quad (4)$$

Thus, to within the constant $\rho_R(E_R)$, the canonical probability (proportional to the microstate density) is represented by the

Laplace transform of the convolution of densities that reduces to the product of individual canonical sums.

In Sec. III, we apply the result for ρ_L to the problem of convolution of nuclear level densities. We show, with the help of an example, that the LT approximation accurately reproduces the convolution density and further investigate the effect of cutting off each of the fragment densities above some threshold energy.

In Sec. IV, we consider changes produced by the introduction of additional degrees of freedom associated with fragment motion. The most important change concerns the function, $\beta(E)$, which characterizes the method and may be thought of as the analog of the inverse temperature that occurs in systems that include a heat reservoir. This function exhibits a nonmonotonic variation that may be interpreted as a change of phase.

In Sec. V, we consider the application of the LT approximation to groups of partitions. It appears to be useful to consider groups of partitions constrained by fixed total mass (charge) and multiplicity (number of fragments). Our objective, in so doing, is to investigate the possibility of expressing statistical weights for all members of a group in Eq. (2). The main difficulty arises because of the fact that, even with fixed mass and multiplicity, a group of partitions exhibits a significant energy fluctuation due to variation of fragmentation Q -values. A simple derivation shows, however, that the induced spread of β values leads to an inaccuracy in partition probabilities that is of the order of 10%. A correction that may be incorporated in a Monte Carlo event generator is proposed and applied in a study (Sec. VI) of the characteristic evolution of the mean values $\langle n_m \rangle$ for a few values of β .

A summary, together with concluding remarks is presented in Sec. VII.

II. LAPLACE TRANSFORM APPROXIMATION FOR THE CONVOLUTION OF DENSITIES

We first make the notion of subsets more precise by considering a finite object that breaks up into a set of fragments that form a partition, \mathbf{n} , of the original object. This step is not essential in the general context but will be useful for discussion of nuclear fragmentation. The k th fragment of the partition is characterized by a density of microstates, $\rho_k(E_k)$. The Laplace transform of the density of states representing a given partition has been given in Eq. (4). Replacing the inverse of the reservoir temperature, T_R , by the generic parameter, b , the inverse transform [the exact convolution density (1)] is written as follows:

$$\rho_{\text{ex}}(E) = \frac{1}{2\pi i} \int_{c-i\infty}^{c+i\infty} \Pi_k \left[\int_0^\infty \rho_k(E_k) e^{-bE_k} dE_k \right] e^{bE} db \quad (5)$$

and is approximated by expanding the logarithm of the integrand in Eq. (5) as a truncated (second order) Taylor series about the maximum. Thus if

$$f(b) = \sum_k \ln \left[\int_0^\infty \rho_k(E_k) e^{-bE_k} dE_k \right] + bE \quad (6)$$

we define the inverse energy β through

$$\left. \frac{df}{db} \right|_{b=\beta} = 0 = E - \sum_k \frac{\int_0^\infty E_k \rho_k(E_k) e^{-\beta E_k} dE_k}{\int_0^\infty \rho_k(E_k) e^{-\beta E_k} dE_k} \quad (7)$$

and write

$$f(b) \approx f(\beta) + \frac{(b-\beta)^2}{2!} \left. \frac{d^2 f}{db^2} \right|_{b=\beta}. \quad (8)$$

Equation (7) simply implies that the sum of the average values of the energies, E_k , is the total energy, E , i.e.,

$$E = \sum_k \langle E_k \rangle. \quad (9)$$

Furthermore, differentiation of Eq. (7) leads (with similar notation) to

$$\left. \frac{d^2 f}{db^2} \right|_{b=\beta} = \sum_k [\langle E_k^2 \rangle - \langle E_k \rangle^2] = \sum_k \sigma_k^2, \quad (10)$$

where, by definition, σ_k^2 is the variance of E_k . With this expansion, the inverse transform [approximation for the convolution, $\rho_{\text{ex}}(E)$] is

$$\rho_L(E) = \frac{e^{f(\beta)}}{2\pi i} \int_{c-i\infty}^{c+i\infty} e^{[\sum \sigma_k^2](b-\beta)^2/2} db, \quad (11)$$

which, with the substitution $b = c + ix$ leads to the following:

$$\rho_L(E) = \frac{e^{\beta E}}{(2\pi \sum_k \sigma_k^2)^{1/2}} x \Pi_k \left[\int_0^\infty \rho_k(E_k) e^{-\beta E_k} dE_k \right]. \quad (12)$$

If the partition involves values of k for which the number of identical fragments, $n_k > 1$, a correction is necessary to avoid counting microstates that represent identical configurations more than once. This ‘‘classical indistinguishability’’ simply entails multiplication of $\rho_L(E)$ by the factor $\Pi_k [1/n_k!]$ [as in Eq. (2)].

For the specific case of fragmentation of a mass M into N fragments we may use the label, m , to designate the masses of constituent fragments. A given partition is then represented as $\mathbf{n} \equiv \{n_1, n_2, \dots, n_m, \dots, n_M\}$, the partition multiplicity, $N = \sum_{m=1}^M n_m$, and the mass, $M = \sum_{m=1}^M m n_m$. In the nuclear case it may be necessary to refer to both the mass and the charge of fragments. This extension is straightforward. We can, however, remark that the simpler forms of the level densities of atomic nuclei depend only on the mass [11].

If we define

$$Z_m = \int_0^\infty \rho_m(E_m) e^{-\beta E_m} dE_m \quad (13)$$

and further set $\sigma^2 = \sum_m \sigma_m^2$, we can write ρ_L corresponding to partitions of fixed mass in the form

$$\rho_L(\mathbf{n}, \beta) = \frac{e^{\beta E}}{(2\pi \sigma^2)^{1/2}} \Pi_m \frac{Z_m^{n_m}}{n_m!} \delta \left(\sum_{m=1}^M m n_m - M \right), \quad (14)$$

where the delta function expresses the mass constraint and the sum of variances, σ^2 , can be considered as a function of β or E depending on the context. In fact, it will be clear

from Eq. (7) that

$$\sigma^2 = -\frac{dE}{d\beta} \quad (15)$$

Equation (14) represents an interesting and important result. For example, we see immediately that, because of the denominator, $\rho_L(\mathbf{n}, \beta)$ is not exactly a product of factors each of which refers only to a particular fragment. We may also observe that, *a priori*, $\beta(E)$ and σ^2 may be partition dependent. Finally, it is useful to note that the analog of the microcanonical inverse temperature is as follows:

$$\frac{d\ln[\rho_L]}{dE} = \beta - \frac{d\ln[\sigma]}{dE} \quad (16)$$

Further development clearly requires a detailed description of the state densities $\rho_m(E_m)$ and therefore depends on the application. We have chosen to study a problem in nuclear reaction physics. Specifically, in the next section (and in fact for the remainder of this work), we are concerned with a simplified form of the nuclear multifragmentation problem.

III. APPLICATION TO NUCLEAR FRAGMENTATION

Let us state immediately that applications of the theory to specific problems may vary considerably with the context. Thus we should keep in mind that the general result is represented by Eq. (14).

That being said, in this section, we examine the specific case of nuclear multifragmentation using a simplified form for nuclear level densities, i.e., for all fragments we assume [3]

$$\begin{aligned} \rho_m(E_m) &= \rho_m(0)e^{2\sqrt{a_m E_m}}, \quad (0 \leq E_m \leq \epsilon_m) \\ &= 0 \text{ otherwise} \end{aligned} \quad (17)$$

In Eq. (17) $\rho_m(0)$ is included for dimensional purposes and may be set to unity and a_m is usually referred to as the level-density parameter. Systematics of the variation of this parameter with nuclear mass were presented by Iljinov *et al.* [12].

The sharp cutoff for each density specified in Eq. (17) is not entirely realistic. It is meant to imply that high excitations correspond to states whose lifetimes are shorter than the characteristic time scale for fragmentation [13]. The introduction of a cutoff has considerable consequences but for the moment it will suffice to notice that the limit of integration in the definition of z_m can be set to ϵ_m . Obviously, in precise practical applications special care should be taken with light nuclei (e.g., nucleons and α particles are usually considered to possess only ground states, and the analytical form of the density may be a poor approximation). However, we may observe that the level density parameter is approximately proportional to the mass number ($a_m \approx m/8$) so that light fragments are not expected to carry important quantities of energy.

Using the densities [Eq. (17)] we have calculated the full convolution microstate density [Eq. (1)] for a partition of mass $M = 125$, $\{n_5 = 1, n_{15} = 1, n_{25} = 1, n_{35} = 1, n_{45} = 1\}$, and compared the result with that obtained using the LT approximation [Eq. (14)]. For these calculations we have assumed the cutoff energies to be proportional to the fragment masses

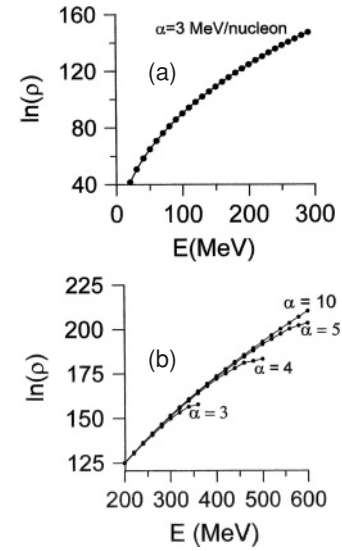


FIG. 1. Density of states (represented as points) obtained by numerical calculation of the density convolution for a “test” partition of mass $M = 125$ $\{n_5 = 1, n_{15} = 1, n_{25} = 1, n_{35} = 1, n_{45} = 1\}$. The calculations were made for a few values of the cutoff parameter, α [defined in Eq. (18)]. The solid lines represent results of calculations using the LT approximation [Eq. (14)]. (a) the low energy region with $\alpha = 3$ MeV/nucleon and (b) higher energies ($\alpha = 3, 4, 5$ and 10 MeV/nucleon) that show the influence of the cutoffs.

so that the cutoffs are specified by the single parameter, α , through

$$\epsilon_m = \alpha m. \quad (18)$$

The result is shown in Fig. 1 for a few values of α . Both the exact and approximate calculations can be made only up to the global cut-off energy αM ([Eq. (7)] has no solution for higher energies). As shown in the figure, the LT approximation is remarkably accurate over a wide range of energies.

IV. INCLUSION OF DEGREES OF FREEDOM ASSOCIATED WITH KINETIC ENERGY

It is, of course, well known [3,10] that the density of states for a partition, $\{n_1, n_2 \dots n_m \dots\}$, involving N fragments confined in a volume, V , with kinetic energy E_k is given by the following:

$$\rho_K(E_K) = \left[V \left(\frac{2\pi}{h^2} \right)^{3/2} \right]^N (\Pi_m m^{3n_m/2}) \frac{E_K^{3N/2-1}}{\Gamma(3N/2)} \quad (19)$$

so that we can define Z_K as a product over fragments

$$Z_K = \int_0^\infty \rho_K(E_K) e^{-\beta E_K} dE_K = \Pi_m (\zeta_m)^{n_m}, \quad (20)$$

where

$$\zeta_m = \frac{V}{h^3} \left[\frac{2\pi m}{\beta} \right]^{3/2}. \quad (21)$$

The inclusion of degrees of freedom associated with kinetic energy of fragments is therefore straightforward (this remains

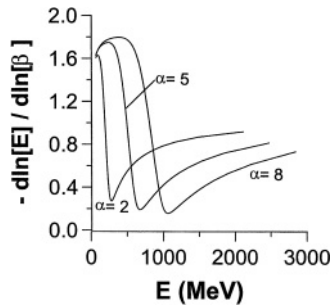


FIG. 2. Effect of the inclusion of kinetic energy [Eq. (19)]. Plot of $-d \ln[E]/d \ln[\beta]$ versus E for a few values of the parameter, α (partition as in Fig. 1). At high energies all curves should tend to the unity. The position of each minimum occurs at an energy that exceeds, by about 10%, the nominal cutoff. This is simply because of the fact that, even in the transition region, a small fraction of the available energy is distributed as fragment kinetic energy.

true when other constraints such as specification of the center of mass are introduced). However it is easy to see that this development profoundly modifies the variation of β near the cutoff simply because we now have [instead of Eq. (13)]

$$E = \sum_m n_m \langle E_m \rangle + \frac{3N}{2\beta} \quad (22)$$

where the second term on the right-hand side represents the mean kinetic energy of N fragments and, following Eq. (13), $\langle E_m \rangle$ refers to the internal excitation energy of the fragment of mass, m . Equation (22) has a solution (with positive β) for all positive values of energy, E . In Fig. 2 we present a plot of the quantity $-d \ln[E]/d \ln[\beta]$ versus E which has the merit of showing, quite clearly, the change of behavior between the low-energy region where β varies approximately as $E^{-1/2}$ to the high-energy region where β is proportional to E^{-1} . This transition is sometimes referred to as a change of phase that, in the present context, is induced by the imposition of cutoffs in the internal energies of fragments resulting in the eventual domination of degrees of freedom associated with fragment motion. We also note that the quantity, σ^2 [Eq. (14) and (15)] receives an additional “kinetic” contribution of $3N/2\beta^2$.

V. PARTITION PROBABILITIES

Let us begin this section with a closer look at the energy that is available to be distributed over “internal” and “kinetic” degrees of freedom for a given partition, (\mathbf{n}) . If the total excitation energy of the parent system is E^* , then this energy is written as follows

$$E(\mathbf{n}) = E^* + \Delta E(\mathbf{n}). \quad (23)$$

The quantity ΔE may include several contributions and is often a substantial fraction of the total energy, E^* . For the sake of simplicity of presentation we assume that

$$\Delta E(\mathbf{n}) = Q(\mathbf{n}), \quad (24)$$

where the Q -value is the energy produced in the fragmentation process leading to the partition, \mathbf{n} . In adopting Eq. (24) we

ignore the influence of the finite size of fragments, [14], and of the interfragment Coulomb interaction energy. Inclusion of this energy (for example, with the help of the Wigner Seitz approximation [5]) is certainly important for precise numerical predictions but does not significantly modify the structure of the formalism. If we write the Q -value as the difference of mass excesses

$$Q(\mathbf{n}) = \Delta(M) - \sum_m n_m \Delta(m), \quad (25)$$

we recover an equation of the form in Eq. (2). Indeed by defining the energy, Γ , through

$$\frac{1}{\Gamma} = \frac{e^{\beta[E^* + \Delta(M)]}}{(2\pi\sigma^2)^{1/2}} \quad (26)$$

and incorporating the kinetic energy via Eq. (21) we arrive at

$$\begin{aligned} \rho_L(\mathbf{n}, \beta) &= \frac{1}{\Gamma} \left\{ \prod_m \frac{[Z_m \zeta_m e^{-\beta \Delta(m)}]^{n_m}}{n_m!} \right\} \delta \left(\sum_{m=1}^M m n_m - M \right) \\ &= \frac{1}{\Gamma} \left\{ \prod_m \frac{X_m^{n_m}}{n_m!} \right\} \delta \left(\sum_{m=1}^M m n_m - M \right), \end{aligned} \quad (27)$$

which defines the parameters

$$X_m = z_m \zeta_m e^{-\beta \Delta(m)}. \quad (28)$$

Note that Eq. (27) is exact within the context of the LT approximation. In particular, provided the Q -value (or its equivalent in more refined theories) can be written as a sum over fragments, the energy, $E(\mathbf{n})$, is accurately represented. However, to apply Eq. (27) to groups of partitions we must allow for the fact that different partitions with different Q -values imply different values of β . In other words, *a priori*, we might suspect that the set of parameters $\{X_m\}$ and the prefactor, $1/\Gamma$, may vary with the partition. It is therefore important to restrict the application to groups of partitions in such a way as to limit the range of Q -values.

A rather severe limitation can be imposed by considering partitions of fixed multiplicity. This is illustrated in the example shown in Fig. 3. From the figure we observe an almost linear dependence of Q on N and, for given N , a typical spread of Q -values with standard deviation about the mean of the order of $\sigma_Q = 20$ MeV. We further observe that this contribution dominates the energy spread (the “partition” variations of the mean values of $\langle E \rangle$ and $\langle \sigma \rangle$ which are produced for groups of partitions at fixed N and β are of the order of the size of the points plotted in the figure).

The existence of significant spread in the values of Q -values thus translates into a corresponding dispersion in the values of β . Therefore if we apply Eq. (27) to groups of partitions in a Monte Carlo event generator and use the values of β and σ corresponding to the average Q -value, i.e., with constant Γ and fixed values of the parameters $\{X_m\}$, it may be necessary to correct generated partition weights for this dispersion. Given Eq. (15) the spread in Q -values corresponds to a variation in β that is typically of the order of 10%. For variations of this order of magnitude values of σ show changes that are typically less than 5% (see Fig. 4). Furthermore, if we ignore for an instant the factor $\sqrt{2\pi\sigma^2}$ in the denominator of

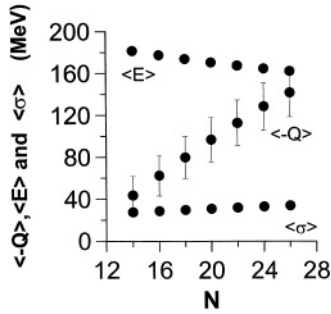


FIG. 3. Results of Monte Carlo calculations (10^7 trials) for groups of partitions with fixed total mass ($M = 125$) and multiplicity, N . The partitions were generated using the multinomial formula [Eq. (2)] in which the set $\{X_m\}$ were calculated using Eq. (28) with the cutoff parameter, $\alpha = 2$ MeV/nucleon and $\beta = 0.2$. The freeze-out volume [Eq. (19)] was taken to be that of a sphere with radius $1.4 \times M^{1/3} = 7$ fm, and the mass excess for each mass corresponds to the isotope with maximum binding energy (for $m > 40$ a fourth-order polynomial fit was used). The “error” bars on the plotted Q -values represent standard deviations of the means $\langle -Q \rangle$.

Eq. (14) we may observe that the value of $b = \beta$ maximizes the partition probability that is thus unaffected by small (first-order) changes in β . If we now reinstate the variation of σ and define the variation of Q -values through

$$Q(\mathbf{n}) = \langle Q \rangle + \Delta Q(\mathbf{n}) \quad (29)$$

we find

$$\Delta \ln[\rho_L(\mathbf{n}, \beta)] = \Delta \beta \frac{d \ln[\sigma]}{d \beta} = \frac{\Delta Q}{\sigma^2} \frac{d \ln[\sigma]}{d \beta}. \quad (30)$$

We shall examine the effect of this correction in the following section, which is concerned with numerical simulations.

VI. CALCULATION OF DISTRIBUTIONS OF AVERAGE PARTIAL MULTIPLICITIES

The main purpose of this section is to exhibit the typical evolution of the mean number of fragments with increasing energy. We also include results of a Monte Carlo generator that is based on Eq. (27) and that, in addition, includes the correction [Eq. (30)]. Explicitly, we consider the evolution of the distribution of mean values, $\langle n_m \rangle$ with β . If the multinomial

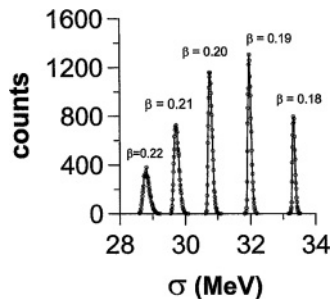


FIG. 4. Distributions of values of σ for multiplicity $N = 20$ obtained using sets of parameters $\{X_m\}$ calculated, using Eq. (28) for a few values of β obtained from Monte Carlo simulations (other parameters as specified in the caption to Fig. 3).

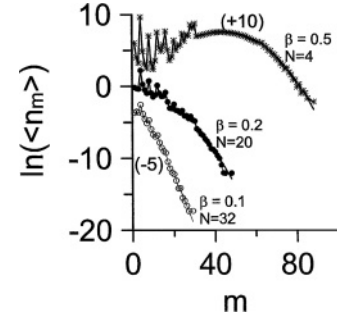


FIG. 5. Evolution of the distributions of the mean partial multiplicities $\langle n_m \rangle$, for values of β ranging from 0.1 to 0.5. The continuous curves [Eq. (31)] are additionally labeled by the values of the multiplicity N corresponding to the maxima of the multiplicity distributions [obtained using Eq. (32)] at each value of β . Plotted points represent the results of Monte Carlo simulations (see text for details).

formula is valid these quantities (and higher order moments) can be easily obtained for partitions of multiplicity, N , using identities given in [1], e.g.,

$$\frac{\langle n_m \rangle}{X_m} = \frac{P(X, N-1, M-m)}{P(X, N, M)} \approx \frac{Q(X, N-1, M-m)}{Q(X, N, M)}, \quad (31)$$

in which $P(N, M)$ is the probability to find partitions with given N, M and $Q(N, M)$ is the same quantity that results from a (two-dimensional) application [1] of the Laplace transform method,

$$\ln[Q(N, M)] = N - \sum_m X_m + a_0 N + a_1 M - \ln[2\pi N \sigma_L]. \quad (32)$$

In Eq. (14) a_0, a_1 , and σ_L are quantities obtained from the set $\{X_m\}$ and the constraints N and M (see Ref. [1] for details).

Figure 5 shows the results of calculations that provide a qualitative picture of the variation of the $\langle n_m \rangle$ distributions with decreasing β (increasing E). The gradual disappearance of fragments of intermediate mass is clearly observed. At $\beta = 0.1$ only light fragments are produced with substantial probability corresponding to the approach to the so-called “vaporization” limit observed in experiment [15].

Superimposed on the curves presented in Fig. 5 are the results of Monte Carlo calculations that were carried out using 10^8 trials with a typical hit rate (corresponding to events with $M = 125$ and N specified as the most probable multiplicity at each value of β) of 2×10^{-3} . As seen in the figure it is difficult to observe any effect due to the correction [Eq. (30)], i.e., the Monte Carlo calculations are in good agreement with the predictions made using equation Eq. (31). This test therefore implies that the multinomial formula is indeed useful for the analysis of multifragmentation partitions although, of course, the importance of the correction may depend to some extent on the observable under consideration.

Given this success it is reasonable to expect that the phase transition may be visible in studies of the kind represented above, i.e., using groups of partitions with fixed multiplicity

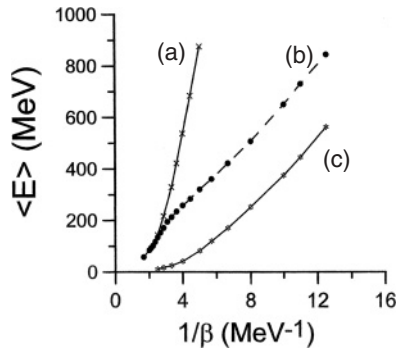


FIG. 6. Monte Carlo calculation of the variation of the average (over partitions) of the energy E with β^{-1} ; (a) with no cutoff ($\alpha = \infty$), (b) $\alpha = 2$ MeV/nucleon (the change of phase is visible as a small “kink” at approximately 200 MeV), and (c) no internal excitation ($\alpha = 0$ MeV/nucleon).

for each value of the total energy, E^* . In Fig. 6 we show a plot of the variation of $\langle E \rangle$ with $1/\beta$ that indicates [curve (b)] that this is indeed the case (this plot is more easily realised than that presented in Fig. 2). The phase change is certainly observed although the signal is somewhat attenuated. Also shown in the figure are the cases with no cutoffs (a) and with the cutoffs set to zero (c) for all nuclei. Despite a regular increase of multiplicity with $\langle E \rangle$ (accompanied by the progressive disappearance of heavy fragments) these two latter cases show no evidence of a transition.

VII. SUMMARY AND DISCUSSION

In this work we have developed the application of the Laplace transform method to the density of microstates represented as a convolution of subsystem densities. The result is expressed in terms of the total excitation energy of the system, E , and a parameter, β , which has the dimension of inverse energy and is closely related to the microcanonical (inverse) temperature. We have specifically considered nuclear multifragmentation and shown, in a case study, that the method furnishes an accurate (and rapidly calculated) representation of the exact result.

We may readily compare the LT approximation with the familiar canonical result. In the canonical formula the temperature is an externally imposed constant, whereas in the LT method the parameter β is determined by the condition that the sum of the mean energies of subsystems is equal to the total energy and is therefore an intrinsic property of a closed system. Both approaches involve a product of factors, each of which is a “Boltzmann weighted” sum of states. However, in the Laplace transform approximation, in contrast with the canonical formula, the parameters, $\{X_m\}$, and the prefactor ($1/\Gamma$) vary with energy (and therefore with the partition). The value of β at each energy is, however, very close to that value that maximizes the partition probability (not exactly because of the factor $1/\sqrt{2\pi\sigma^2}$) resulting in a relative insensitivity of partition probabilities to small changes in β (not true in the canonical approximation).

The inclusion of degrees of freedom corresponding to kinetic energy highlights the existence of a transition that occurs when the total excitation energy exceeds the maximum energy that can be accommodated as internal excitation energy of fragments. This transition can reasonably be thought of as a change of phase and is accompanied by a qualitative evolution of the morphology of partitions that occur with significant probability. At energies below the cutoff region the density of microstates is maximized for partitions with small Q -values (typically those partitions with small multiplicities), whereas at high energies the increase in multiplicity favors the predominant production of small fragments (high multiplicity partitions). It is important to note, however, that this latter “multiplicity driven” evolution does not in itself signal a transition because it is not uniquely engendered by a finite cutoff. This study thus indicates that one should look for the transition in the function $E(\beta)$.

Our analysis also suggests that it should be possible, at least in nuclear multifragmentation, to delimit groups of partitions each group being characterized by average values of β and σ in which case we arrive at the familiar multinomial form (i.e., at a formal analogy with the canonical result). In this situation it should still be possible to detect the transition that takes place when the internal excitation energy saturates.

-
- [1] A. J. Cole, Phys. Rev. C **69**, 054613 (2004).
 - [2] Y. Suzuki and K. Varga, *Stochastic Variational Approach to Quantum Mechanical Few-Body Problems* (Springer-Verlag, Heidelberg, 1998).
 - [3] A. J. Cole, *Statistical Models for Nuclear Decay* (IOPP, Bristol, 2000).
 - [4] J. Richert and P. Wagner, Phys. Rep. **350**, 1 (2001).
 - [5] J. P. Bondorf, A. S. Botvina, A. S. Iljinov, I. N. Mishustin, and K. Sneppen, Phys. Rep. **257**, 133 (1995).
 - [6] D. H. E. Gross, *Microcanonical Thermodynamics* (World Scientific, Singapore, 2001), Vol. 66.
 - [7] P. Désesquelles, Phys. Rev. C **65**, 034604 (2002).
 - [8] A. J. Cole, P. J. Lindstrom, H. J. Crawford, and B. G. Harvey, Phys. Rev. C **39**, 891 (1989); A. J. Cole *et al.*, Z. Phys. A **356**, 171 (1996); A. J. Cole and P. Désesquelles, *ibid.* **337**, 71 (1990).
 - [9] L. G. Moretto, R. Ghetti, L. Phair, K. Tso, and G. J. Wozniak, Phys. Rep. **287**, 249 (1997).
 - [10] W. Greiner, L. Neise, and H. Stocker, *Thermodynamics and Statistical Mechanics* (Springer-Verlag, Heidelberg, 1995), Chap. 7.
 - [11] T. Ericson, Adv. Phys. **9**, 423 (1960).
 - [12] J. Iljinov, E. De Sanctis, C. Guaraldo, V. Lucherini, V. Muccifora, E. Polli, A. R. Reolon, and P. Rossi, Nucl. Phys. **A543**, 517 (1992).
 - [13] M. G. Mustafa, M. Blann, A. Ignatuk, and S. M. Grimes, Phys. Rev. C **45**, 1078 (1992).
 - [14] A. J. Cole, D. Heuer, and M. Charvet, Phys. Rev. C **55**, 2978 (1997).
 - [15] M. F. Rivet *et al.*, Phys. Lett. **B388**, 219 (1996); B. Borderie *et al.*, *ibid.* **B388**, 224 (1996).